HST/ACS SnapShot Imaging of 29 Post-Starburst Quasars

S. L. Cales[1], M. S. Brotherton[1], Z. Shang[1], N. Bennert[2], G. Canalizo[3], R. Stoll[4], R. Ganguly[1], D. Vanden Berk[5], C. Paul[6], and A. Diamond-Stanic[7]

ABSTRACT

WORK - Wait for results

We present quantitative host galaxy measurements of 29 post-starburst quasars (PSQs) from a Hubble Space Telescope (*HST*) Advanced Camera for Surveys (ACS) Wide Field Channel (WFC) Snapshot program. PSQs are broad-lined AGN that also possess the spectral signatures of massive, moderate-aged stellar populations (in excess of ten billion solar masses and ages of hundreds of Myrs). The PSQs were selected from the Brotherton et al. (2008a, in preparation) catalog to have SDSS $r < 18.6$, Hδ absorption equivalent widths > 1 Å, $0.25 < z < 0.45$ (ensuring high luminosity and similar sizescales, resolving structures a half Kpc across) focusing on the clearest most luminous ($\langle M_r \rangle \sim -22.7$) examples of PSQs. The aim of our study is to test the hypothesis that PSQs are an intermediate phase in the life of a quasar/galaxy. To this end we characterize the morphologies, bulge luminosities and quasar to host galaxy light contributions via two-dimensional image analysis of the PSF subtracted images. We look for trends between the host galaxy measurements and the morphology classifications. The *HST*/ACS-F606W (broad V-band at 0.05"/pixel) SNAP images show that while some of the PSQs are obviously quasars living in spiral galaxies, others appear to be disturbed ellipticals inviting us to classify the PSQs as undisturbed spirals, merger or post-merger events. In two of the images we see obvious merging and about 40% have neighbors within $10''$. The vast majority of systems show signs of interaction/merger activity, such as, tidal tails, shells, star-forming knots and asymmetries. These results are consistent with merging scenarios which build larger elliptical galaxies via mergers of smaller spiral ones.

---

[1]University of Wyoming, Laramie, WY 82071

[2]University of California, Santa Barbara, CA 93106

[3]University of California, Riverside, CA 92521

[4]Ohio State University, Columbus, Ohio 43210

[5]Pennsylvania State University, University Park, PA 16802

[6]University of California, Davis, CA 95616

[7]University of Arizona,Tucson, AZ 85721

1. Introduction

Some two decades ago the search for what lurks at the centers of galaxies was spawned by the argument that quasars existed in overwhelmingly larger numbers at $z \gtrsim 2$ than now, thus the answer was expected to be dead quasar engines. Observational results have shown that massive galaxies harbor supermassive black holes (BHs) at their centers (Kormendy & Richstone 1995) and that the properties of these host galaxies correlate with the black hole mass. Specifically, there exists a tight correlation between the masses of these black holes and that of the host galaxy stellar bulge component ($M_{BH} \sim 0.15\%\ M_{bulge}$; Magorrian et al. 1998; Gebhardt et al. 2000a), or measured from the stellar velocity dispersion with a tighter correlation (M-σ_* relation; Gebhardt et al. 2000b; Ferrarese & Merritt 2000; Tremaine et al. 2002). This M_{BH}-M_{bulge} relation suggests that the growth of black holes is intimately linked to the formation and evolution of their host galaxies and hints at their originating via a common physical process which synchronizes the growth of both (Kauffmann & Haehnelt 2000; Granato et al. 2004; Hopkins et al. 2008). In the current epoch we can hope to learn about the formation and evolution of BHs and their host galaxies by understanding how the properties of both relate.

According to the standard cosmology, hierarchical merging is responsible for the formation of larger galaxies via mergers of smaller ones ('merger hypothesis'; Toomre 1977). Additionally, the triggering of major starburst is attributed to mergers, possibly accounting for the growth of supermassive black holes and the formation of quasars, and ultimately predicting the formation of many of the structures that we see in the Universe today.

Circumstantial evidence via observations and theoretical modeling support the 'merger hypothesis'. Ultraluminous infrared galaxies (ULIRGs), strongly interacting merger systems heated by both starburst and AGN power sources, have been hypothesized to evolve into normal quasars after the central engine clears away the dust associated with the massive star formation (Sanders et al. 1988; Sanders & Mirabel 1996; Veilleux 2006). These objects are possibly the first observational step in the evolution and formation of a larger elliptical galaxy. Post-starburst galaxies show signs of fossil AGN feedback and are thought to be evolved galaxies after a few 100 Myr after the peak of star formation and AGN activity (Tremonti, Moustakas, & Diamond-Stanic 2007). Furthermore, the host galaxies of "normal" quasars have been found to be disturbed (e.g., Canalizo & Stockton 2001; Kauffmann et al. 2003; Canalizo et al. 2007; Bennert et al. 2008), a telltale sign of interaction, and reveal the presence of young stellar populations (e.g., Brotherton et al. 1999; Canalizo & Stockton 2001; Kauffmann et al. 2003; Jahnke et al. 2004; Vanden Berk et al. 2006). These distinct phenomenological phases are theoretically part of an evolutionary merger timeline (Hopkins et al. 2008).

Numerical simulations have enjoyed great success in reproducing the physical properties of elliptical galaxies and bulges through major mergers of gas-rich disk galaxies (Granato et al. 2004; Di Matteo et al. 2005; Hopkins et al. 2006). These simulations follow star formation and BH growth simultaneously during gas-rich galaxy-galaxy collisions and find that mergers lead to strong gaseous

inflows that feed the quasar and intense starbursts (ULIRG phase). In due course, feedback energy released by the quasar, "blowout", quenches both star formation and further black hole growth (Di Matteo et al. 2005). Without further star formation the blue remnant quickly evolves to a red galaxy (blue to red sequence). Thus, AGN feedback is deemed responsible for (among other things) the coupling of the BH mass with the host bulge mass as well as the bimodality of the color distribution of galaxies.

Still there are other possibilities which could lead to both black hole growth and bulge growth (e.g.,minor mergers, harassment, bars, instabilities). At lower levels these phenomenon are expected to contribute to the this growth however we propose that it is not the fundamental mechanism responsible for the M-σ_* relation.

An object at "blowout" would be expected to have luminous quasar activity, starburst or post-starburst signatures along with indications of a recent merger (e.g.,companion, tidal tails, star forming knots, asymmetries...). UN J1025-0040, upholds many features of the evolutionary theory. The post-starburst quasar (PSQ) prototype, UN J1025-0040 is hosted by a galaxy with a ∼400 Myr old strong starburst (Brotherton et al. 1999), the host appears as a merger remnant (Brotherton et al. 2002), and has a companion galaxy in a post-starburst phase (Canalizo et al. 2000). A younger UN J1025-0040 (tens of Myrs after the starburst) would have a more luminous stellar population and would likely be dust-enshrouded, placing it in the ULIRG class. These observations suggest that UN J1025-0040 is a plausible transition between ULIRGs and quasars (Brotherton et al. 1999).

PSQs are predicted to be a phase in the life of a quasar/galaxy at or around "blowout" and thus, the "smoking gun" evidence for AGN feedback showing how the M_{BH}-σ_* correlation arises. This paper is the first in a multi-dimensional series of papers devoted to understanding the properties of PSQs. Our aim for this paper is to characterize the morphology and other host galaxy parameters of a sample of 29 PSQs via *HST*/ACS-F606W Snap imaging. Selection of the sample and data used in this paper are discussed in § 2. The PSQs are characterized via two-dimendional analysis and visual inspection in § 3. In § 4 we discuss degree of disturbance and host galaxy properties as a function morphology along with how these characterizations align with other types of galaxies (e.g., post-starburst galaxies, quasars). In § 5 we summarize our conclusions. We choose a flat universe in which H_o is 71 km^{-1}s^{-1}Mpc and Ω_M equal to 0.27.

2. Data

2.1. Experimental Design and Sample Selection

PSQs are a rare class of objects. Of the over 50,000 quasars found by Sloan Digital Sky Survey data release 3 (SDSS DR3; Schneider et al. 2002) ∼600 were spectroscopically selected and catalogued by Brotherton et al. (2008a, in preparation; hereafter B8a) as PSQs. The automated selection algorithm was primarily based on that of Zabludoff et al. (1996), an algorithm used to

select post-starburst galaxies. The selection criteria required that the spectra display both the broad emission lines of luminous AGNs (Seyfert galaxies or quasars) and the Balmer jumps and high-order Balmer absorption lines of massive stellar populations on order of hundreds of Myr old.

Focusing on the clearest most luminous ($\langle M_r \rangle \sim -22.7$) examples of PSQs a subsample of 80 PSQs from the B8a catalogue was chosen for request from *HST*'s Snap program. We received 29 *HST*/ACS-F606W (broad V-band at $0.05''$/pixel) SNAP images. The PSQs were selected from the B8a catalog to have SDSS $r < 18.6$, Hδ absorption equivalent widths > 1 Å, $0.25 < z < 0.45$ (ensuring high luminosity and similar sizescales, resolving structures a half Kpc across). The sample of 29 will hereafter be referred to as the *HST* sample.

2.2. Observations and Data Reductions

ACS Wide Field Channel (WFC) snapshot observations for this program (proposal ID 10588: PI M. Brotherton) were carried out during Cycle 14 between July 2005 and November 2006. Of the 80 PSQs in our target list, 29 were observed. For each field, two 360s F606W images, offset by a pixel shift in each direction, were acquired in order to facilitate the removal of cosmic rays and hot pixels. The F606W filter ($\Delta\lambda = 2342$Å; 1 pixel corresponds to $0.05''$) corresponds to the rest frame B of the sample, strategically used in order to probe the higher-order Balmer absorption lines and Balmer jump. The images were calibrated "on the fly" as they were retrieved from the *HST* archive site. The final images were downloaded from the *HST* archive in 2008 July to ensure the most consistent and updated calibrations.

Table 1. *HST* Sample Observations

SDSS Name	z	M_r	*HST* Obs Date
J003043−103517	0.296	-23.236	05 Nov, 2006
J005739+010044	0.253	-22.603	11 Jun, 2006
J020258−002807	0.339	-22.418	16 Oct, 2005
J021447−003250	0.349	-22.952	03 Dec, 2005
J023700−010130	0.344	-23.096	11 Oct, 2005
J040210−054630	0.27	-22.395	07 Aug, 2005
J074621+335040	0.284	-23.321	03 Jan, 2006
J075045+212546	0.408	-23.064	15 Dec, 2005
J075521+295039	0.334	-22.741	08 Dec, 2005
J075549+321704	0.42	-22.819	27 Oct, 2005
J081018+250921	0.263	-22.289	10 Dec, 2005
J105816+102414	0.275	-22.531	22 Jan, 2006
J115159+673604	0.274	-22.051	13 Aug, 2005
J115355+582442	0.319	-22.144	19 Aug, 2005
J123043+614821	0.324	-22.113	17 Mar, 2006
J124833+563507	0.266	-22.938	31 Jul, 2005
J145640+524727	0.277	-22.079	15 Aug, 2005
J145658+593202	0.326	-22.549	12 Jul, 2006
J154534+573625	0.268	-23.096	28 Oct, 2005
J164444+423304	0.317	-22.978	10 Mar, 2006
J170046+622056	0.276	-22.14	12 Feb, 2006
J210200+000501	0.329	-23.193	24 May,2006
J211343−075017	0.42	-23.029	06 Jun, 2006
J211838+005640	0.384	-23.207	03 Jun, 2006
J212843+002435	0.346	-22.93	17 Jul, 2005
J230614−010024	0.267	-21.887	06 Jun, 2006
J231055−090107	0.364	-23.32	19 Aug, 2005
J233430+140649	0.363	-22.603	22 Jul, 2006
J234403+154214	0.288	-21.896	10 Jun, 2006

2.3. PSF Subtraction

We use a PSF to model the AGN/quasar core of a PSQ where the residual contains only galaxy/host contribution. We utilized a number of ways to generate a PSF for subtraction. In § 2.3.1, 2.3.2 and 2.3.3 we describe the methods used to generate PSFs for the *HST* images. In GALFIT the fitting functions/light distributions are convolved with the PSF to simulate blurring cause by the telescope optics and/or the atmosphere.

2.3.1. PCA - ???

2.3.2. Tiny Tim

According to the newest simulations of AGN-to-host decomposition (Kim et al. 2008) PSF variations are caused by three general conditions: temporal variations, position on the detector and to a lesser extent the source SED. With this in mind we generate a library of candidate PSFs using Tiny Tim (Version 6.3). The library spans parameter space in three-dimensions: PSF diameter, location in the image and jitter. The PSF diameters range from 1 to 15 arcseconds in one arcsecond increments. The location in x, y pixel coordinates is chosen to be that which matches the target coordinates. Lastly, jitter is chosen to be either set to none or 7 milliarcseconds to simulate telescope breathing and detector effects. The power law $F_\nu = \nu^\alpha$ where $\alpha = -0.3$ (Bennert et al. 2008) is adopted for all PSFs.

2.3.3. "Real" Star

We followed the prescription set forth by Canalizo et al. (2007) for the observed PSF star which we describe briefly here. The star was chosen from the *HST* archive and processed in a standard manner. The PSF was then adaptively smoothed by comparing the data to the standard deviation s of the sky, according to the following: i) for data of high signal ($> 7s$), the PSF was unmodified; ii) for values between $3s$ and $7s$, a Gaussian kernel of $\sigma = 0.5$ pixel was used to smooth the image, iii) for data of $< 3s$ we used a Gaussian kernel of $\sigma = 2.0$ pixels and finally, iv) after this last step if then the data values were $< 1s$ the value was replaced by zero.

3. Results

3.1. Two-Dimensional Image Analysis

GALFIT (Peng et al. 2002) is a 2-dimensional fitting program utilizing chi-squared minimization to simultaneously fit components in an image having different light distributions (e.g., sky,

PSF, de Vaucouleurs (de Vaucouleurs 1948), Sérsic (Sérsic 1968)...). The Sérsic power law is a generalized power law defined by

$$\Sigma(r) = \Sigma_e \exp\left[-\kappa\left(\left(\frac{r}{r_e}\right)^{1/n} - 1\right)\right]. \quad (1)$$

The pixel surface brightness at the effective radius r_e is Σ_e. The effective radius is defined such that half of the flux is within r_e and constrains k to be coupled to the Sérsic index, n. The Sérsic index, also called the concentration index, describes the shape or concentration of the brightness profile. A large index gives a steeply sloping profile towards small radii with extended wings. Conversely, small values of n have shallow inner profiles with steep truncation at large radius. Special cases of the Sérsic power law are the exponential ($n = 1$) and de Vaucouleurs ($n = 4$) used to fit the disk and bulge of galaxies, respectively.

We decompose the image to determine the quasar to host light fraction, host morphology and other host parameters. The method is as follows. We created a mask to exclude the surrounding objects. As suggested by Peng et al. (2002) we begin simply by fitting a PSF (as found by the methods of § 2.3) simultaneously with the sky. We then test a number of different fits: i) Sérsic, ii) Exponential, iii) de Vaucouleurs, iv) Sérsic plus Sérsic, v) Sérsic plus Exponential, vi) Sérsic plus de Vaucouleurs and the fit is then recalculated. The modeled components are all centered on the position of the QSO.

Now - Present Sérsic fitted images, table, histogram; Near Future - Finish all PSF sizes, with S, E, D, S+E, S+D, S+S, present fitted images, table, histogram

- Images
  - Rerun on original images
  - B&W?
  - crop out dynamic scale
  - label with SDSS names
  - where is N?
  - size scale?
  - ISSUES: 02 and 14

- Table - Modeling Results
  - Format?
  - r_{eff} => $''$ or kpc

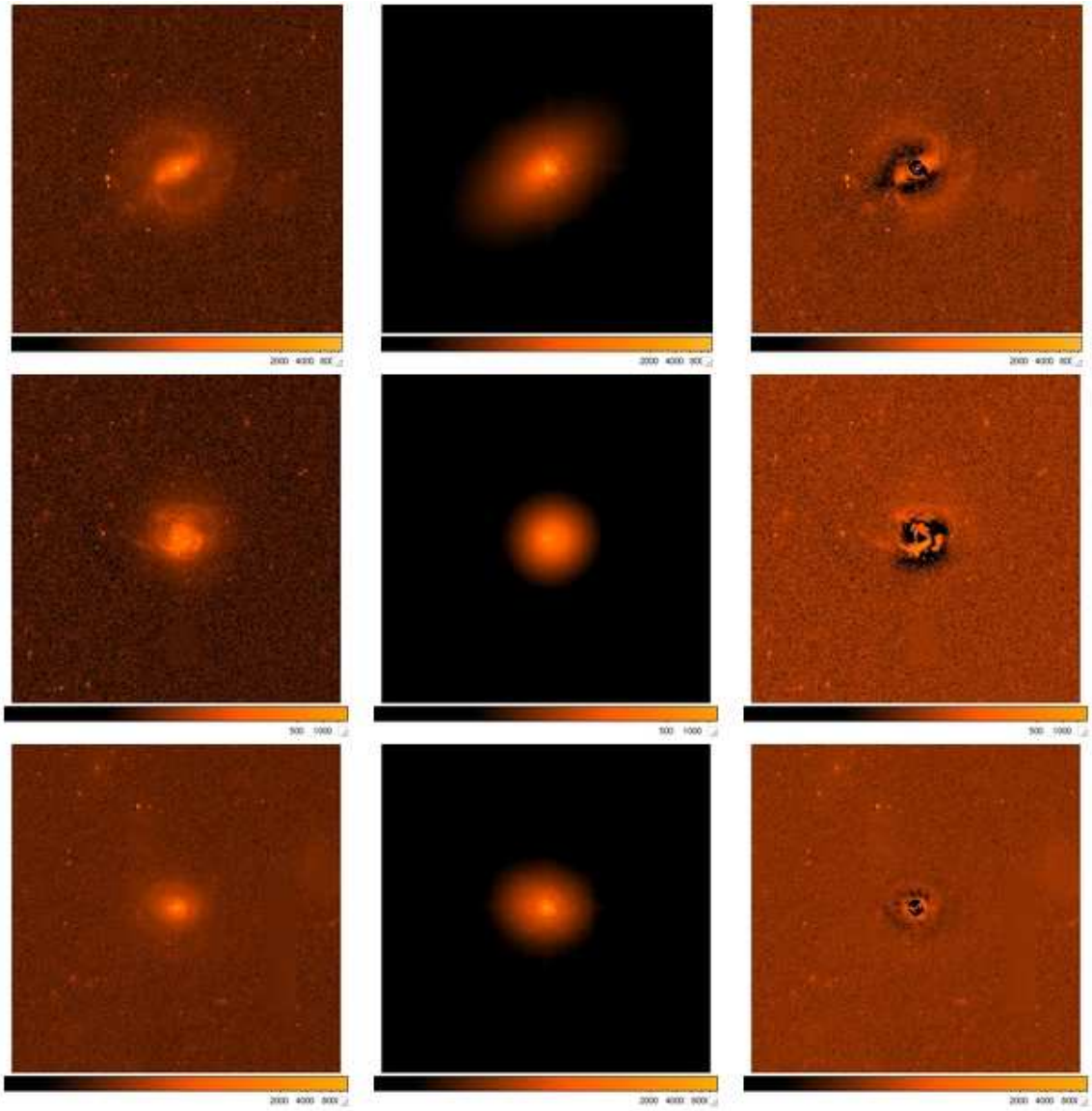

Fig. 1*a*

Fig. 1.— Raw (*left*), GALFIT model (*middle*) and residual (*right*) images of the PSQs. The images are $20''\times\ 20''$.

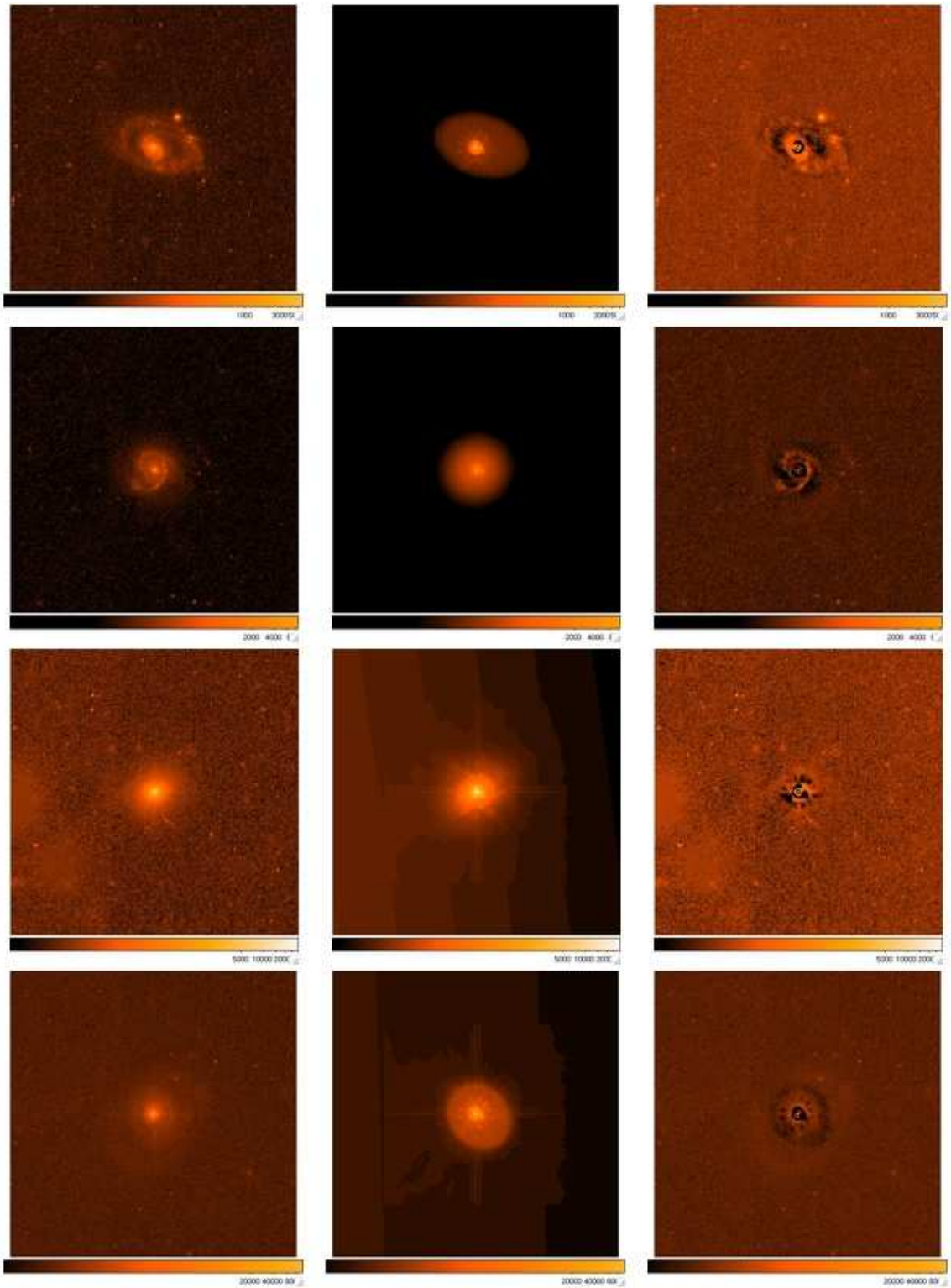

Fig. 1*b*

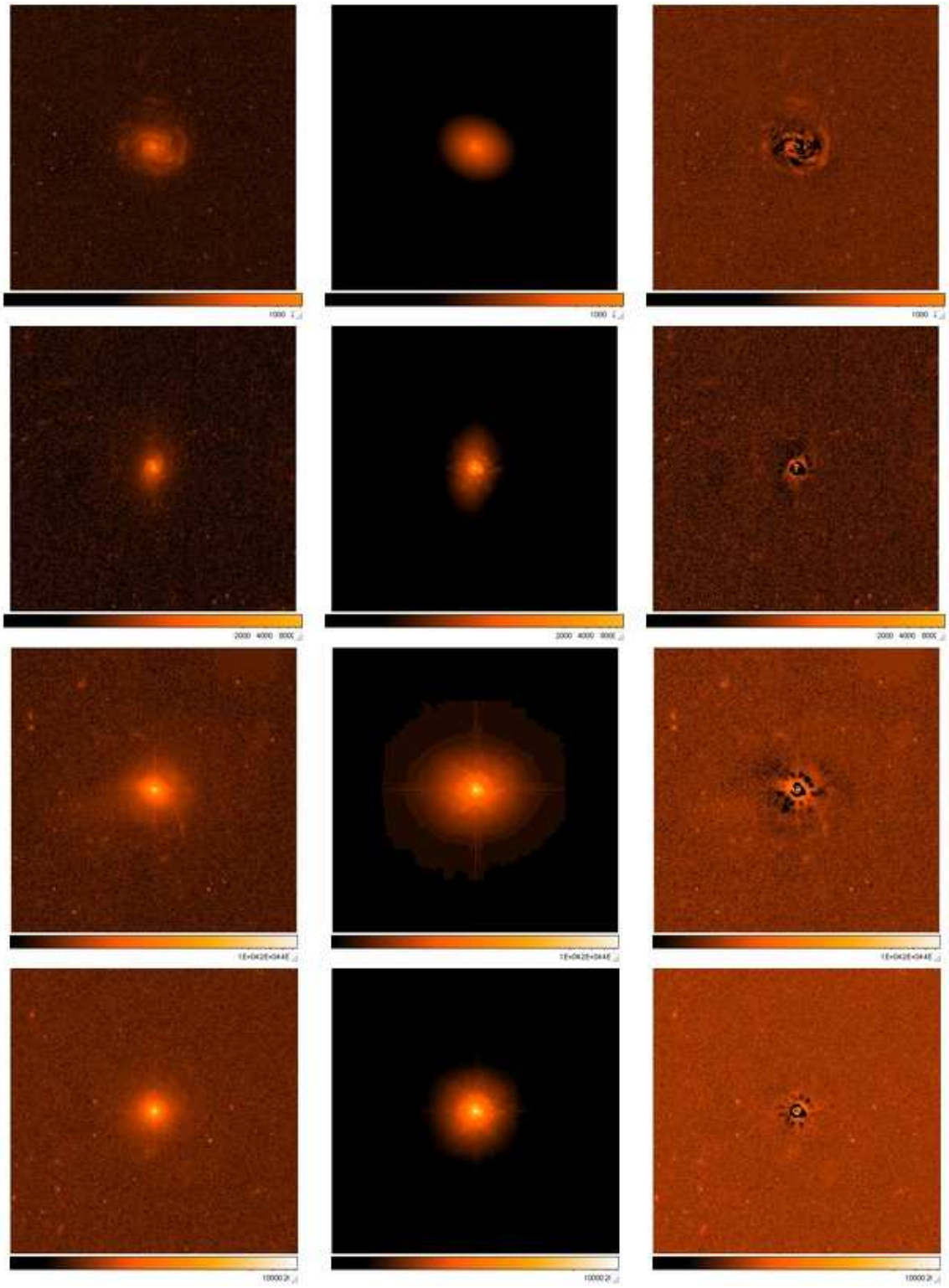

Fig. 1*c*

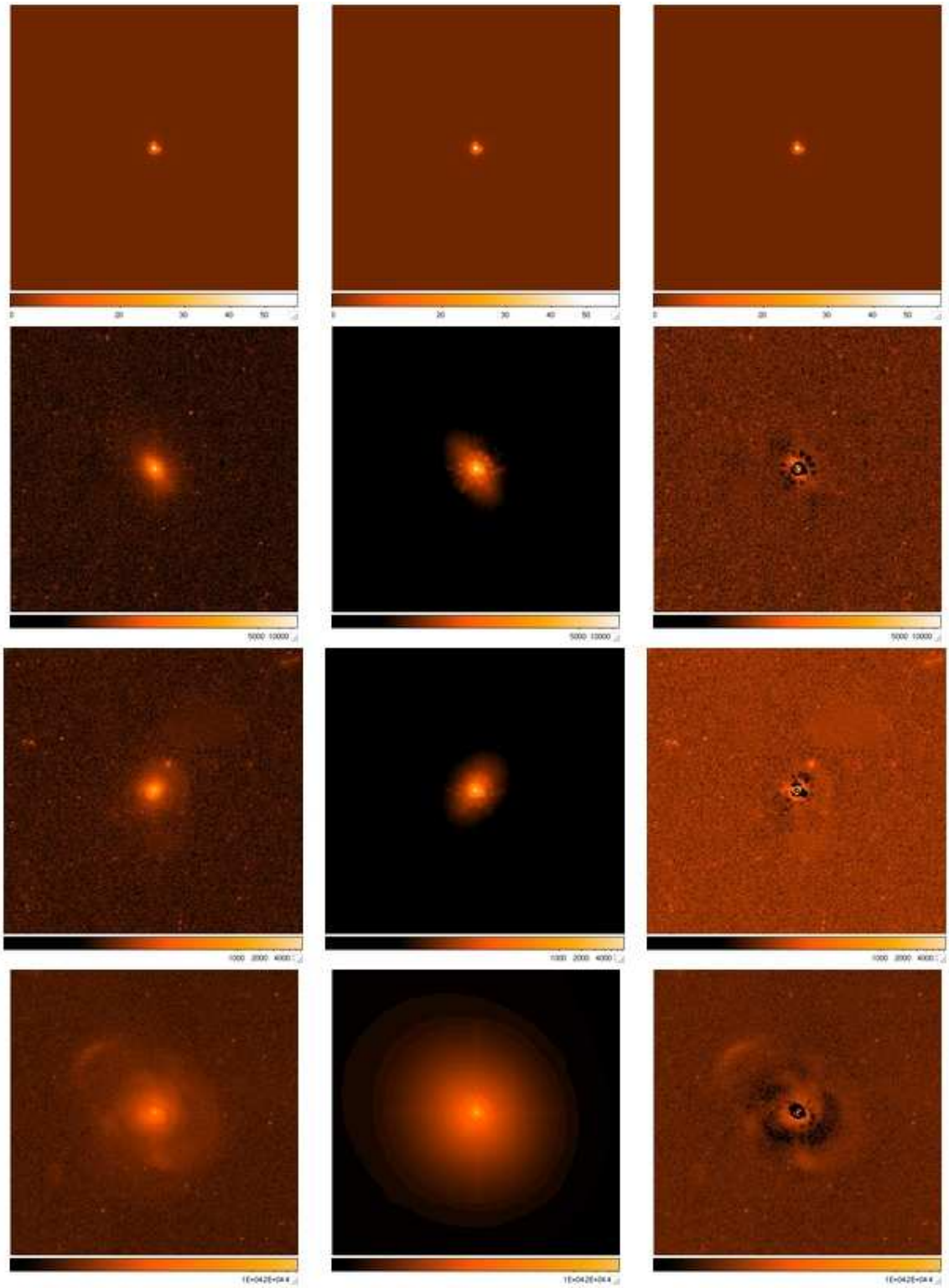

Fig. 1*d*

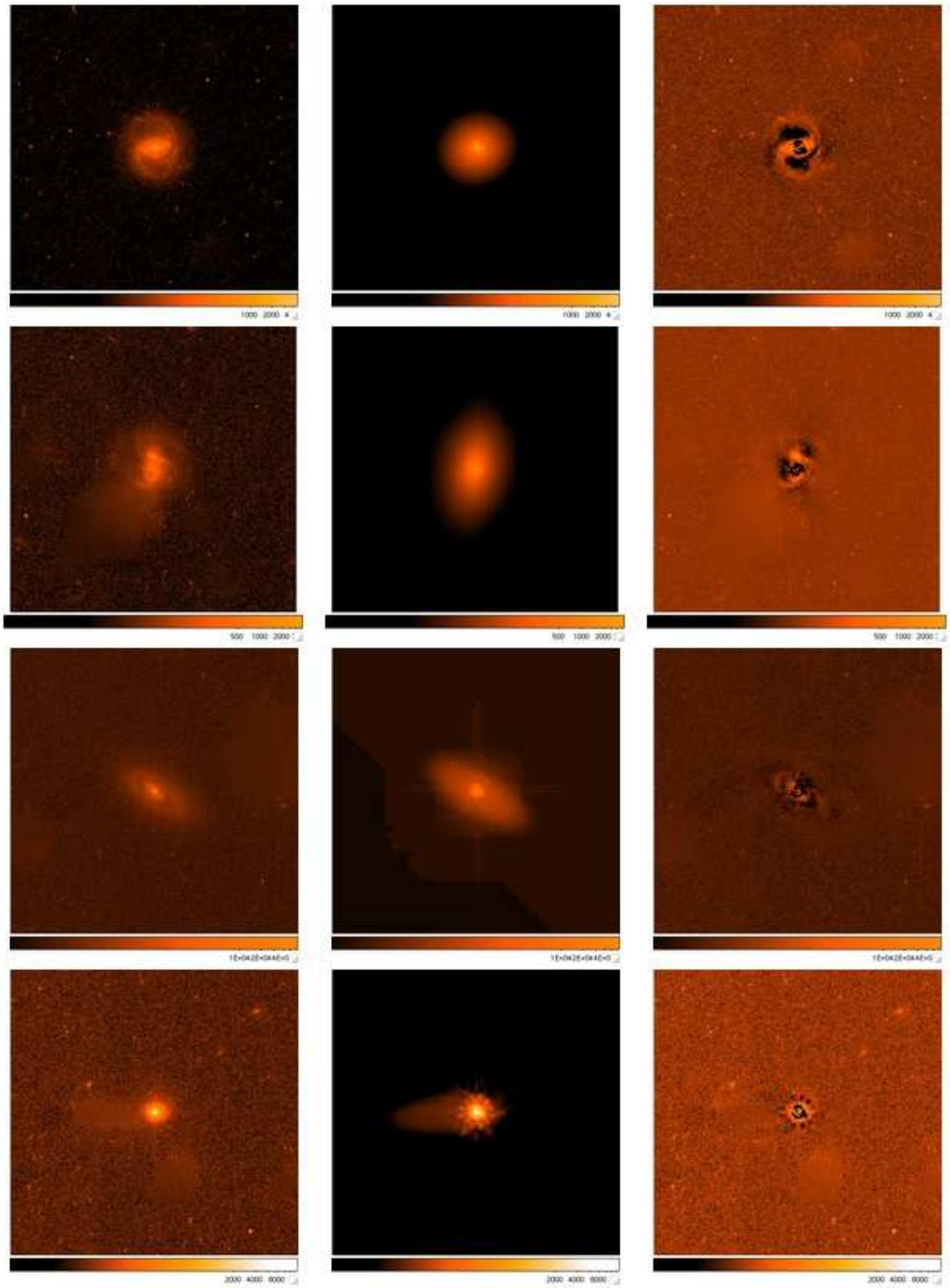

Fig. 1*e*

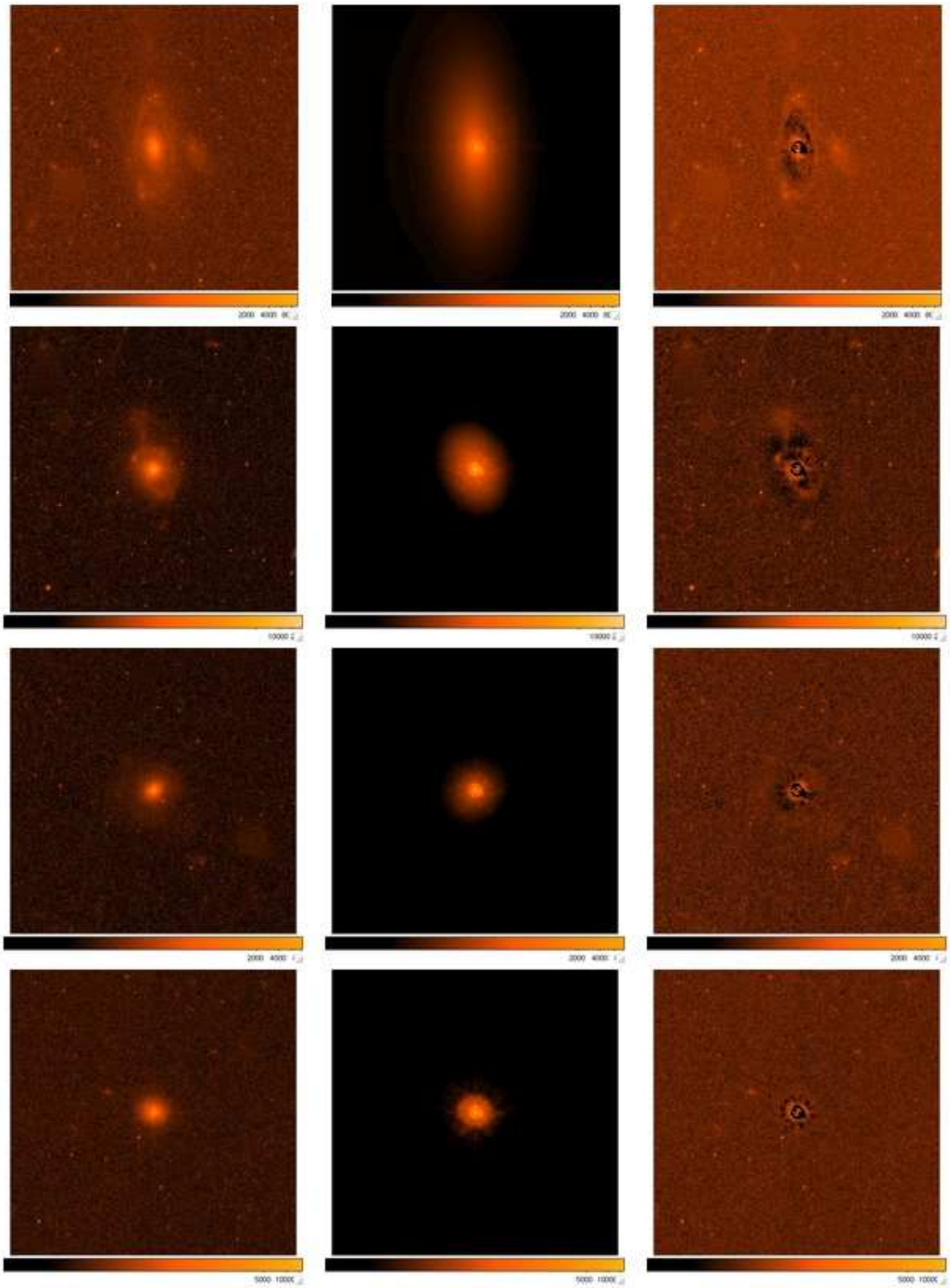

Fig. 1*f*

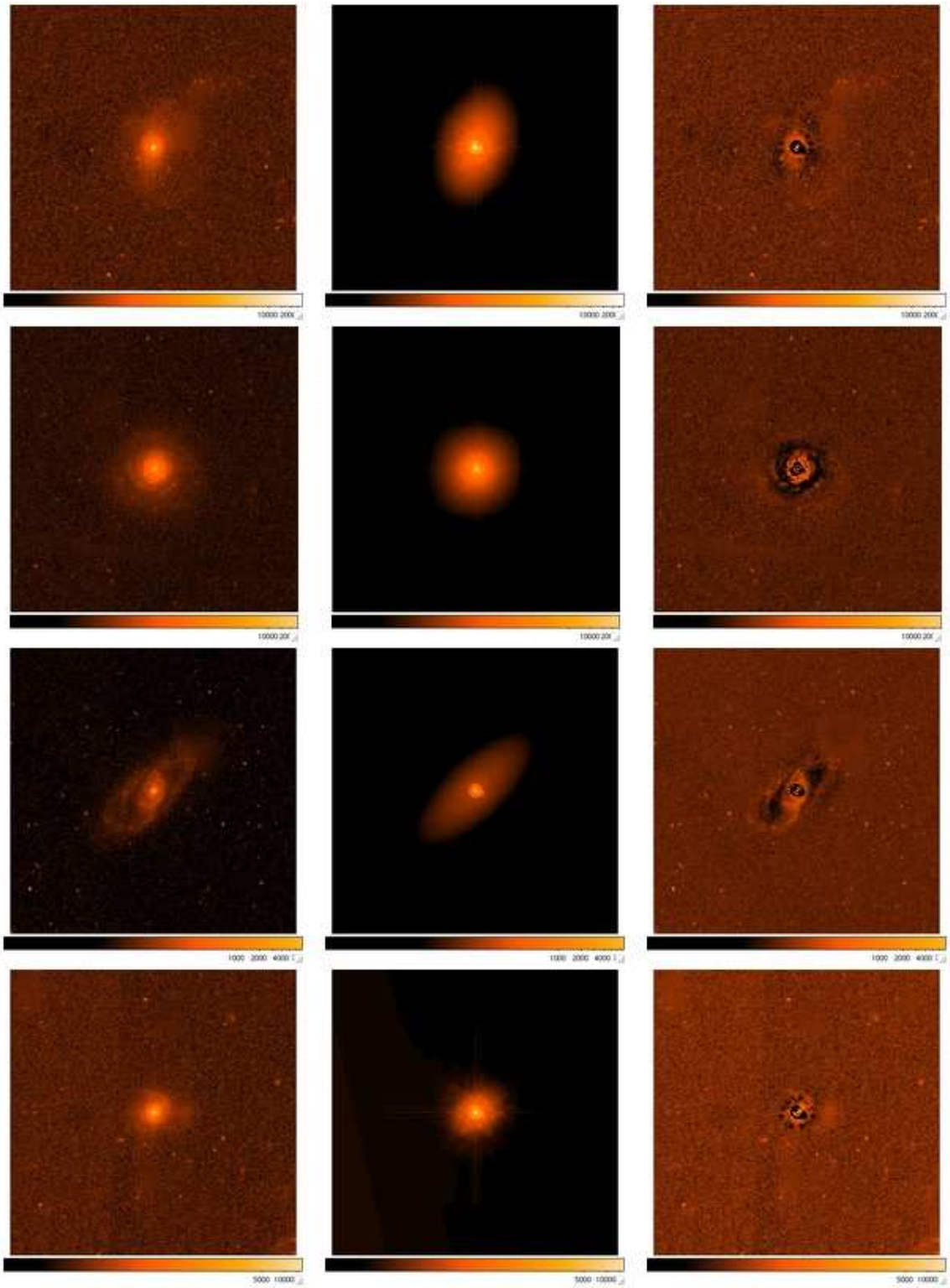

Fig. 1*g*

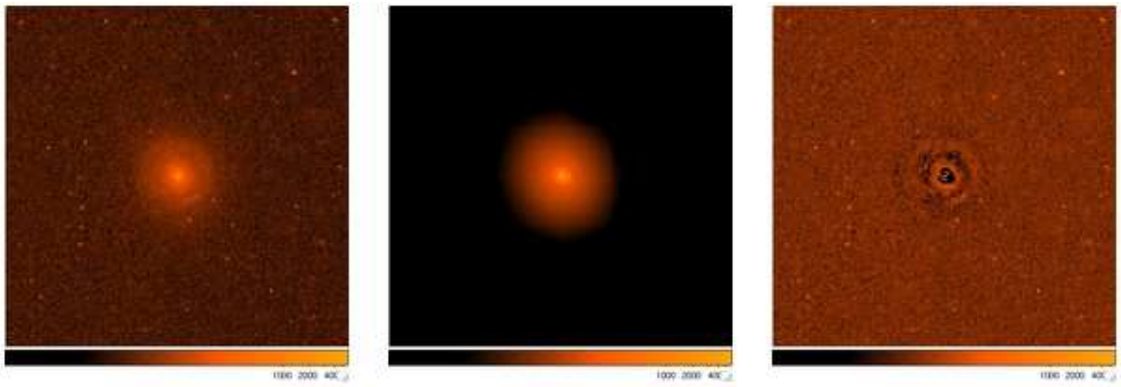

Fig. 1*h*

Table 2. PSQ Host Galaxy Modeling Results

SDSS Name	PSF	Sérsic Component					χ^2_ν
	$m_{\rm F606W}$ (mag)	$m_{\rm F606W}$ (mag)	r_{eff} (pixels)	n	b/a	P.A. (°)	
J081018+250921	18.2	19.3	33.18	1.3302	0.7726	-86.43	32.79
J124833+563507	18.9	18.3	45.55	1.398	0.9081	38.33	30.31
J230614−010024	19.2	18.8	19.26	1.431	0.9271	-29.85	27.6
J154534+573625	18.9	19.5	38.57	0.3555	0.4281	58.43	28.89
J040210−054630	20.7	19.7	24.24	0.53	0.9519	-54.47	23.33
J115159+673604	18.5	20.0	4.3	2.	0.3	0.	23.33
J105816+102414	19.2	19.5	16.25	2.7471	0.94	-23.71	22.78
J170046+622056	20.2	19.4	59.27	2.3402	0.4327	3.401	25.81
J145640+524727	19.9	19.2	25.88	0.7702	0.8906	-64.23	22.03
J074621+335040	19.0	19.7	11.54	2.7163	0.6638	-59.55	25.35
J234403+154214	20.2	19.4	31.46	0.698	0.8841	26.83	32.14
J003043−103517	19.6	19.3	41.16	1.9649	0.5656	-53.27	30.93
J164444+423304	19.3	21.9	51.19	0.1992	0.347	-83.25	22.2
J115355+582442	19.1	20.8	33.4	0.8323	0.4426	30.87	30.75
J123043+614821	19.4	19.9	36.1	2.0982	0.6052	-32.39	35.33
J145658+593202	21.1	19.3	29.03	1.4292	0.5583	-9.316	17.39
J210200+000501	19.4	20.0	31.09	0.5613	0.6888	19.83	27.26
J075521+295039	21.2	19.4	22.22	0.7798	0.7944	65.77	28.3
J020258−002807	20.9	19.1	17.18	1.0145	0.9567	-55.23	28.78
J023700−010130	19.7	20.1	45.3	0.1069	0.6279	73.51	35.21
J212843+002435	19.8	20.3	38.83	0.6257	0.5853	-17.73	25.13
J021447−003250	19.6	20.1	24.66	0.6526	0.7783	80.72	24.51
J233430+140649	19.4	21.2	20.92	0.3235	0.7692	-51.36	23.04
J231055−090107	20.2	19.4	65.08	0.482	0.3919	-46.32	31.72
J211838+005640	19.4	21.1	15.45	0.0608	0.8536	66.61	28.24
J075045+212546	18.8	20.4	40.67	0.0311	0.8488	38.66	47.24
J211343−075017	19.7	20.6	20.62	1.2162	0.8715	-42.28	24.1
J075549+321704	19.7	20.7	28.82	1.0291	0.5002	-7.094	26.44

- Histogram - Fig-6 fromGuyon2006ApJ166-89 - Nice

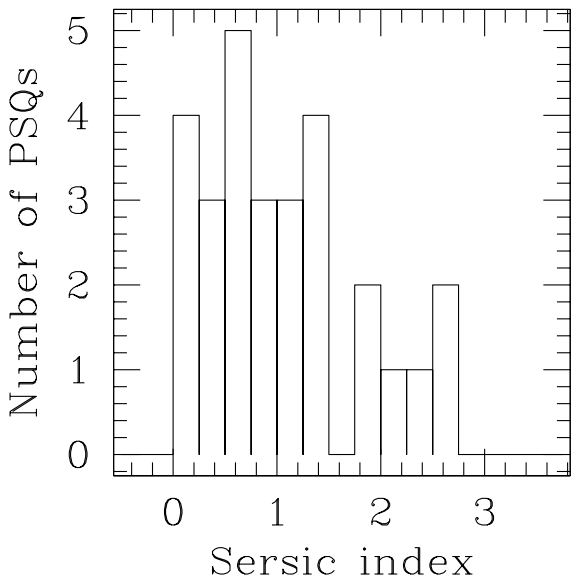

Fig. 2.— Fig-6 fromGuyon2006ApJ166-89 - Nice

3.2. Morphologies and Companions

Table 3. PSQ Host Morphologies Tab-5 fromGuyon2006ApJ166-89 - Table form of descriptions below

SDSS Name	Visual				χ^2_ν Model	Adopted Type	Notes
	Morphology	Bar	Arm(s)	Disturbance			
J003043−103517	ᔓ	✓	✓				
J005739+010044	ᔓ		✓				Asymmetric
J020258−002807	?			!			Asymmetric, SF arc
J021447−003250	⬭						
J023700−010130	ᔓ		✓	!			Ring, SF knot
J040210−054630	?			✓			Tidal tail/Intersecting companion?
J074621+335040	⬭						
J075045+212546	⬭			✓			Shells
J075521+295039	ᔓ		✓				Asymmetric
J075549+321704	ᔓ	✓	✓				
J081018+250921	⬭			✓			
J105816+102414	⬭						
J115159+673604	ᔓ	✓	✓				
J115355+582442	⬭						
J123043+614821	?			?			
J124833+563507	⬭			!			Shells
J145640+524727	ᔓ	✓	✓				Asymmetric, Fine structure
J145658+593202	ᔓ?			!			Merger of 2-3 ᔓ
J154534+573625	ᔓ?						
J164444+423304	⬭						
J170046+622056	ᔓ			✓			Ring, Dust lane, Merging companion
J210200+000501	⬭			✓			Tidal tail
J211343−075017	⬭						Companion
J211838+005640	⬭						
J212843+002435	⬭						Companion
J230614−010024	ᔓ		✓?				Single arm, Tidal features, Companion
J231055−090107	ᔓ		✓	✓			Merging companion
J233430+140649	⬭			✓			Tidal feature
J234403+154214	ᔓ						

Structure of following paragraphs: OBJECT SDSS NAME - i) Host galaxy morphology, ii) Fit results, iii) Other references, iv) Apparent companions.

SDSS J003043.59-103517.6 – The host is of barred spiral type viewed face-on with two symmetric spiral arms clearly visible. Three distinct cases of fuzz are located within about 10″(WNW, NE and SSE). There is a companion galaxy at the same redshift 14.″7 from the central nucleus (PA = 146°).

SDSS J005739.19+010044.9 – This host is a slightly asymmetric face-on spiral.

SDSS J020258.94−002807.5 – Classification of the host is not apparent. The object, having an arc in the SE quadrant of the object 0.″8 from the nucleus of asymmetric star formation, is clearly disturbed.

SDSS J021447.00−003250.6 – This object appears to be a fairly smooth elliptical.

SDSS J023700.30−010130.5 – This ring galaxy reveals spiral-like structure in the nucleus. A bright structure of the ring (likely a star forming knot) is visible 2.″6 to the SSW (PA = 211°).

SDSS J040210.90−054630.3 – The target here appears to have undergone recent interaction. It could be that this is a spiral with a bright star-forming tidal tail in the east. However, what looks like a tidal tail could (and may well) be the remnant of an intersecting companion galaxy. A ring of star formation appears in the NW quadrant of the object at a line of sight semi-major axis distance of 1.″2.

SDSS J074621.06+335040.7 – The target appears to be a smooth elliptical.

SDSS J075045.00+212546.3 – The host appears to be an elliptical with possible interation/merger signatures visible in the form of shells (one such shell is apparent in the NE quadrant of the target at a line of sight radius of 3.″7).

SDSS J075521.30+295039.2 – The arms of this spiral are flocculent and asymmetric.

SDSS J075549.56+321704.1 – Although at first glance this object might appear to be an elliptical, a closer look reveals a faint bar (in comparison to the glare of the AGN) of length 0.″9 oriented in the SE-NW axis. A companion of this object (14.″6 from target, PA = 140°) is visually disturbed with a jagged 'S' appearance and long tidal tail extending toward the north.

SDSS J081018.67+250921.2 – A faint hint of a tidal tail/fuzz emanating from the central SE quadrant towards the south (3.″5, PA = 136°) adds fine structure to this otherwise smooth elliptical host.

SDSS J105816.81+102414.5 – This host appears to be a smooth elliptical.

SDSS J115159.59+673604.8 – Two symmetric, yet faint spiral arms connect via the bar (4.″9 across, SE-NW axis) of this face-on barred spiral. (SDSS photometrically identifies a neighboring galaxy 15.″6 from the target at PA = 104°).

SDSS J115355.58+582442.3 − The object appears to be a smooth elliptical elongated in the ENE-WSW axis. (SDSS photometrically identifies a neighboring galaxy 16.″3 from the target at PA = 325°).

SDSS J123043.41+614821.8 − Classification of the host is ambiguous. The host shows faint flocculent spiral structure without revealing anything so organized as arms. (SDSS photometrically identifies a neighboring galaxy 2.″0 from the target at PA = 164°).

SDSS J124833.52+563507.4 − This elliptical can be characterized as anything but smooth. Flare-like shells are at large in the NW and SE quadrants of the object (radii = 4.″4 and 6.″1, respectively) as well as a visible dust-lane within a line of sight distance 0.″5 from the quasar in a NNW-SSE fashion. (SDSS photometrically identifies a neighboring galaxy (which appears to be a spiral) 16.″7 from the target at PA = 92°).

SDSS J145640.99+524727.2 − This host is a face-on barred (2.″2 across, NNE-SSW axis) spiral with fine structure. (SDSS photometrically identifies a fuzzy neighboring galaxy 8.″2 from the target at PA = 297°).

SDSS J145658.15+593202.3 − Merger of 2-3 spiral (?) galaxies with another apparent spiral companion within 9.″7 at PA = 213. The double nuclei are less than 1.″0 apart, which is in turn 4.″1 from the galaxy approaching from the west (PA = 90°). (SDSS photometrically recognizes several other galaxies within 10.″0).

SDSS J154534.55+573625.1 − This is an ambiguous object. At first glance one might classify the host as an elliptical. But, on closer inspection there appears to be a flattened disk, elongated in the ENE-WSW direction and a dust lane that envelopes the nucleus 1.″3 (line of sight) in the semi-major axis and 0.″6 (line of sight) in the semi-minor axis. (SDSS photometrically identifies a fuzzy neighboring galaxy 9.″3 from the target at PA = 133°).

SDSS J164444.92+423304.5 − The host appears to be a smooth elliptical. (SDSS photometrically identifies what appears to be an edge-on spiral along with another spiral at distances, 3.″0 (PA = 0°) and 4.″5 (PA = 107), respectively, from the target.)

SDSS J170046.95+622056.4 − The disk of this spiral has a ring of star formation 3.″6 (or a dust lane at 2.″, semi-major axis line of sight) from the central source. This ring of star formation is presumably be due to harassment as a small satellite galaxy prepares to merge 2.″6 (line of sight, PA = 197°) with the large spiral. (SDSS photometrically identifies a fuzzy neighboring galaxy 6.″3 from the target at PA = 45°).

SDSS J210200.42+000501.8 − This elliptical has a tidal tail extending 4.″1 (PA = 264°) in length from the central source possibly wrapping around behind the host (from W to E) and ending with the tip of the tail on the opposite side of origin at a distance of 4.″1 (PA = 80°). The fuzz, which we call the tip of the tail, is at the same redshift as the host.

SDSS J211343.20-075017.6 − The smooth elliptical target is at a line of sight distance of 7.″5

(PA = 132°) from its elliptical companion.

SDSS J211838.12+005640.6 – The object appears to be a smooth elliptical.

SDSS J212843.42+002435.6 – This elliptical, which is elongated in the NE-SW direction has (what appears to be an elliptical) companion located 2.″6 (PA = 162°) from the central source.

SDSS J230614.18-010024.4 – The companion of this flocculent face-on spiral is 10.″8 (line of sight, PA = 246°) from the nucleus. The host appears to have a single arm (which could be a tidal tail) located in the NE quadrant of the object, as well as a tidal arc 1.″7 from the nucleus in the SE.

SDSS J231055.50-090107.6 – One arm of this spiral extends in the north while the companion galaxy gnaws on the southern arm at a line of sight center to center distance of 4.″1 (PA = 212°).

SDSS J233430.89+140649.7 – This object appears to be a fairly smooth elliptical with a faint tidal tail disturbance in the SE quadrant.

SDSS J234403.55+154214.0 – The host is similar to that of *SDSS J230614.18−010024.4*: a flocculent face-on spiral.

4. Discussion & Conclusions - Add ALL!

- Comparisons to PSGal (other galaxy types) - e.g., Tab-6 McLeod and McLeod2003ApJ590-707
- Simple robust statements
  - Qualitative => Interacting Galaxies - Characterize/order as (use galfit to help):
    - Harassment
    - Mergers (Current vs Residual)
    - Singular (No interaction)
  - Quantitative (quasar to stellar fractions):
    - SDSS - spectral
    - HST - true
  - Bulge Component - from GALFIT results for M-sigma
  - Certain Age (starburst & quasar) - picked to be a certain age (100s Myr) then how come so diverse?
- Compare Morphology with properties

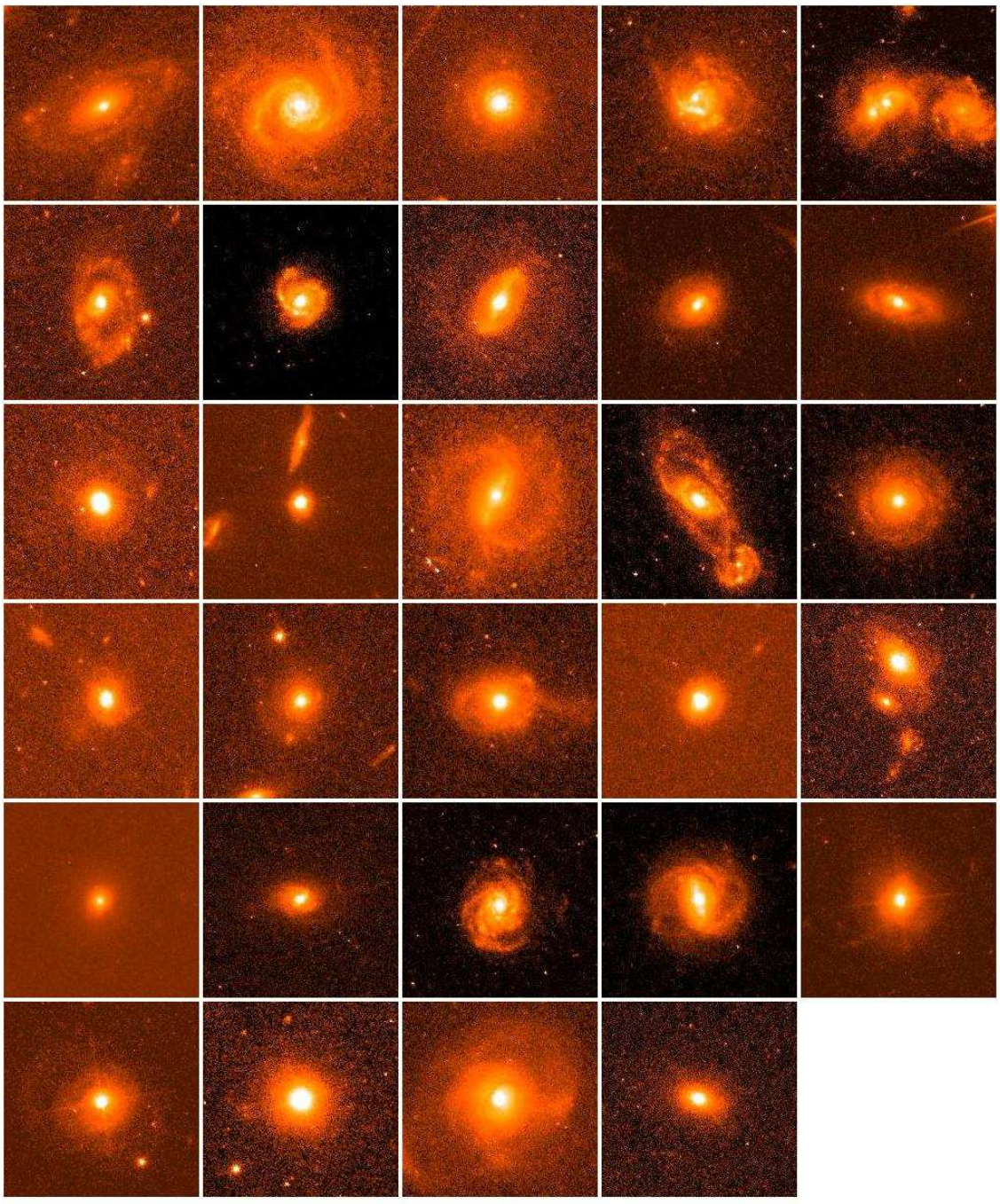

Fig. 3.— Where? A mosaic of the 29 *HST*/ACS images. Each image is 10″× 10″and NE is towards the upper left. At *HST's* high resolution (∼0.05″) and an average redshift of $\langle z \rangle \sim 0.319$, these 200 × 200 pixel images correspond to about 46.7 kpc across. We choose a flat universe in which H_o is 71 km/s/Mpc and Ω_M equal to 0.27. See also `http://phsics.uwy.edu/agn/psq/index.html` for a finer detailed view.

5. Summary - Last

...

6. Outline

- Abstract - WORK - Wait for results
- 1. Introduction - Mehh...!?!
  - M_{BH} vs. M_{bulge} Correlation - OK
    - M_{BH} vs. M_{bulge} Correlation ...
    - Evolution connection - process/mechanism synchronize/truncate/couple, "By understanding how the properties of BHs relate to those of their host galaxies, we can hope to learn about the formation and evolution of both."
  - 'Merger hypothesis'/Hierarchical merging - S + S − > E!
  - Support for mergers
    - Circumstantial - Observations
      - ULIRG − > PSG − > Quasar − > Elliptical
      - Phenomena part of theoretical timeline
    - Simulations (w/ feedback, Theoretical evidence) - Springel et al. 2005, bimodal distribution, terminate SF abruptly
      - Reproduce observed physical properties
      - "Blowout"/AGN feedback - mechanism ∼simultaneously quench SF and BH growth
      - Explains - M-sigma and red sequence
  - Other possibilities
  - Objects During Feedback
    - The First PSQ, UN J1025-0040 (Prototype) - properties
    - Prototype - evolution
  - Conclusion of Intro
    - Hypothesis
    - Outline
    - Cosmology
- 2. Data
  - 2.1 Experimental Design and Sample Selection

    - ¶1 PSQ intro - OK
    - ¶2 HST Sample/Design - OK
  - 2.2 Observations and Data Reductions
    - HST - OK
    - Table - OK
  - 2.3 PSF Subtraction
    - 2.3.1 HST PCA - ???
    - 2.3.2 HST Tiny Tim - OK
    - 2.3.3 HST "Real" - OK

- 3. Results
  - 3.1 Two-Dimensional Image Analysis - HST 2-D Analysis - Now - Present Sérsic fitted images, table, histogram; Near Future - Finish all PSF sizes, with S, E, D, S+E, S+D, S+S, present fitted images, table, histogram
    - Images
      - Rerun on original images
      - B&W?
      - crop out dynamic scale
      - label with SDSS names
      - where is N?
      - size scale?
      - ISSUES: 02 and 14
    - Table - Modeling Results
      - Format?
      - r_{eff} => $''$ or kpc
    - Histogram - Fig-6 fromGuyon2006ApJ166-89 - Nice
  - 3.2 Morphologies and Companions
    - Tab-5 fromGuyon2006ApJ166-89 - Table form of descriptions
    - Add in i) Fit results, and ii) Other references (if nec)

- 4. Discussion and Conclusions - Add ALL!
  - Comparisons to PSGal (other galaxy types) - e.g., Tab-6 McLeod and McLeod2003ApJ590-707
  - Simple robust statements
    - Qualitative => Interacting Galaxies - Characterize/order as (use galfit to help):
      - Harassment

        - Mergers (Current vs Residual)
        - Singular (No interaction)
      - Quantitative (quasar to stellar fractions):
        - SDSS - spectral
        - HST - true
      - Bulge Component - from GALFIT results for M-sigma
      - Certain Age (starburst & quasar) - picked to be a certain age (100s Myr) then how come so diverse?
  - Compare Morphology with properties

- 5. Summary - Last

REFERENCES

Bennert, N., Canalizo, G., Jungwiert, B., Stockton, A., Schweizer, F., Peng, C. Y., & Lacy, M. 2008, ApJ, 677, 846

Brotherton, M., Stoll, R., Paul, C., Diamond-Stanic, A., Shang, Z., Cales, S., Ganguly, R., Canalizo, G., & Vanden Berk, D. 2008a, ApJ

Brotherton, M. S., Grabelsky, M., Canalizo, G., van Breugel, W., Filippenko, A. V., Croom, S., Boyle, B., & Shanks, T. 2002, PASP, 114, 593

Brotherton, M. S., van Breugel, W., Stanford, S. A., Smith, R. J., Boyle, B. J., Miller, L., Shanks, T., Croom, S. M., & Filippenko, A. V. 1999, ApJ, 520, L87

Canalizo, G., Bennert, N., Jungwiert, B., Stockton, A., Schweizer, F., Lacy, M., & Peng, C. 2007, ApJ, 669, 801

Canalizo, G. & Stockton, A. 2001, ApJ, 555, 719

Canalizo, G., Stockton, A., Brotherton, M. S., & van Breugel, W. 2000, AJ, 119, 59

Di Matteo, T., Springel, V., & Hernquist, L. 2005, Nature, 433, 604

Ferrarese, L. & Merritt, D. 2000, ApJ, 539, L9

Gebhardt, K., Bender, R., Bower, G., Dressler, A., Faber, S. M., Filippenko, A. V., Green, R., Grillmair, C., Ho, L. C., Kormendy, J., Lauer, T. R., Magorrian, J., Pinkney, J., Richstone, D., & Tremaine, S. 2000a, ApJ, 539, L13

Gebhardt, K., Kormendy, J., Ho, L. C., Bender, R., Bower, G., Dressler, A., Faber, S. M., Filippenko, A. V., Green, R., Grillmair, C., Lauer, T. R., Magorrian, J., Pinkney, J., Richstone, D., & Tremaine, S. 2000b, ApJ, 543, L5

Granato, G. L., De Zotti, G., Silva, L., Bressan, A., & Danese, L. 2004, ApJ, 600, 580

Hopkins, P. F., Hernquist, L., Cox, T. J., & Kereš, D. 2008, ApJS, 175, 356

Hopkins, P. F., Hernquist, L., Cox, T. J., Robertson, B., & Springel, V. 2006, ApJS, 163, 50

Jahnke, K., Sánchez, S. F., Wisotzki, L., Barden, M., Beckwith, S. V. W., Bell, E. F., Borch, A., Caldwell, J. A. R., Häussler, B., Heymans, C., Jogee, S., McIntosh, D. H., Meisenheimer, K., Peng, C. Y., Rix, H.-W., Somerville, R. S., & Wolf, C. 2004, ApJ, 614, 568

Kauffmann, G. & Haehnelt, M. 2000, MNRAS, 311, 576

Kauffmann, G., Heckman, T. M., Tremonti, C., Brinchmann, J., Charlot, S., White, S. D. M., Ridgway, S. E., Brinkmann, J., Fukugita, M., Hall, P. B., Ivezić, Ž., Richards, G. T., & Schneider, D. P. 2003, MNRAS, 346, 1055

Kim, M., Ho, L. C., Peng, C. Y., Barth, A. J., & Im, M. 2008, ArXiv e-prints, 807

Kormendy, J. & Richstone, D. 1995, ARA&A, 33, 581

Magorrian, J., Tremaine, S., Richstone, D., Bender, R., Bower, G., Dressler, A., Faber, S. M., Gebhardt, K., Green, R., Grillmair, C., Kormendy, J., & Lauer, T. 1998, AJ, 115, 2285

Peng, C. Y., Ho, L. C., Impey, C. D., & Rix, H.-W. 2002, AJ, 124, 266

Sanders, D. B. & Mirabel, I. F. 1996, ARA&A, 34, 749

Sanders, D. B., Soifer, B. T., Elias, J. H., Neugebauer, G., & Matthews, K. 1988, ApJ, 328, L35

Schneider, D. P., Richards, G. T., Fan, X., Hall, P. B., Strauss, M. A., Vanden Berk, D. E., Gunn, J. E., Newberg, H. J., Reichard, T. A., Stoughton, C., Voges, W., Yanny, B., Anderson, S. F., Annis, J., Bahcall, N. A., Bauer, A., Bernardi, M., Blanton, M. R., Boroski, W. N., Brinkmann, J., Briggs, J. W., Brunner, R., Burles, S., Carey, L., Castander, F. J., Connolly, A. J., Csabai, I., Doi, M., Friedman, S., Frieman, J. A., Fukugita, M., Heckman, T. M., Hennessy, G. S., Hindsley, R. B., Hogg, D. W., Ivezić, Ž., Kent, S., Knapp, G. R., Kunzst, P. Z., Lamb, D. Q., Leger, R. F., Long, D. C., Loveday, J., Lupton, R. H., Margon, B., Meiksin, A., Merelli, A., Munn, J. A., Newcomb, M., Nichol, R. C., Owen, R., Pier, J. R., Pope, A., Rockosi, C. M., Saxe, D. H., Schlegel, D., Siegmund, W. A., Smee, S., Snir, Y., SubbaRao, M., Szalay, A. S., Thakar, A. R., Uomoto, A., Waddell, P., & York, D. G. 2002, AJ, 123, 567

Toomre, A. 1977, in Evolution of Galaxies and Stellar Populations, ed. B. M. Tinsley & R. B. Larson, 401–+

Tremaine, S., Gebhardt, K., Bender, R., Bower, G., Dressler, A., Faber, S. M., Filippenko, A. V., Green, R., Grillmair, C., Ho, L. C., Kormendy, J., Lauer, T. R., Magorrian, J., Pinkney, J., & Richstone, D. 2002, ApJ, 574, 740

Tremonti, C. A., Moustakas, J., & Diamond-Stanic, A. M. 2007, ApJ, 663, L77

Vanden Berk, D. E., Shen, J., Yip, C.-W., Schneider, D. P., Connolly, A. J., Burton, R. E., Jester, S., Hall, P. B., Szalay, A. S., & Brinkmann, J. 2006, AJ, 131, 84

Veilleux, S. 2006, New Astronomy Review, 50, 701

Zabludoff, A. I., Zaritsky, D., Lin, H., Tucker, D., Hashimoto, Y., Shectman, S. A., Oemler, A., & Kirshner, R. P. 1996, ApJ, 466, 104